A Multibody Model of an Ornithopter

Article *in* Journal of Guidance, Control, and Dynamics · January 2009

DOI: 10.2514/1.43177

CITATIONS
54

READS
1,264

2 authors:

Jared Grauer
National Aeronautics and Space Administration
88 PUBLICATIONS **1,186** CITATIONS
SEE PROFILE

James Edward Hubbard Jr.
University of Maryland, College Park
105 PUBLICATIONS **2,730** CITATIONS
SEE PROFILE

47th AIAA Aerospace Sciences Meeting Including The New Horizons Forum and Aerospace Exposition
5 - 8 January 2009, Orlando, Florida

AIAA 2009-727

A Multibody Model of an Ornithopter

Jared A. Grauer* and James E. Hubbard Jr.†
Department of Aerospace Engineering, University of Maryland, College Park, MD, 20742

Flapping-wing aircraft which mimic avian flight gaits, or ornithopters, are becoming increasingly popular as the size of avionics hardware shrinks amidst the persistent demand for smaller and more efficient flight vehicles. The development of an accurate model of the associated flight dynamics provides insight into the relevant physics and facilitates the use of simulation, system identification, and feedback control techniques. Analysis of inertial properties and previous flight data has led to the development of a multibody model, where the ornithopter is modeled as a collection of chains of rigid body linkages emanating from a central fuselage. The Boltzmann-Hamel equations of motion are employed to generate a state space model which is cast into a form canonical to the nonlinear robotics and adaptive control communities. Software implementation of the symbolic derivation and numerical integration of the equations of motion are discussed. Preliminary results are presented for the simulation of the ornithopter in straight and level flight using a simplified aerodynamics model, which illustrate the trends in measured flight data.

Nomenclature

$\mathbf{C}(\mathbf{p},\mathbf{v})$	dynamic coupling matrix	$\mathbf{u}$	control input
C, K	center of mass and coordinate frame	$\mathbf{v}$	generalized velocity
C_t, C_d, C_l	aerodynamic force coefficients	$\mathbf{x}$	state vector
$\mathbf{E}(\mathbf{p},\mathbf{v})$	environmental forces	$\mathbf{z}$	axis of rotation
$\mathbf{e}$	unit vector	α	angle of attack
$\mathbf{f}$	force	$\boldsymbol{\eta}$	orientation
$\mathbf{g}$	gravitational acceleration	$\boldsymbol{\theta}$	joint angles
$\mathbb{I}$	identity matrix	$\boldsymbol{\nu}$	translational velocity
$\mathbf{I}$	inertia tensor	$\boldsymbol{\omega}$	angular velocity
$\mathbf{J}_f$	forcing Jacobian	$\otimes$	Kronecker product
$\mathbf{J}_K$	kinematic Jacobian	$\times$	cross product
$\mathbf{J}_\eta$	rotational Jacobian	$\|.\|$	Euclidean norm
$\mathbf{l}$, $\mathbf{r}$	joint locations		
$\mathbf{M}(\mathbf{p})$	generalized mass matrix	*Subscripts*	
m	mass	x, y, z	orthonormal frame projections
N	system degrees of freedom	$(.)_{ij}$	description at i relative to j
N_j	links on chain j	$(.)_{ij}$	link i of chain j
N_k	number of kinematic chains	$\{.\}_{ij}$	matrix elements
$\mathbf{p}$	generalized position		
$\mathbf{R}$	rotation matrix	*Superscripts*	
$\mathbf{r}$	position vector	$(.)^i$	tensor expressed in frame K_i
$\mathbf{S}(.)$	skew operator	^{T}	transpose
T	kinetic energy	$\dot{.}$	time derivative
t	time		
U	potential energy		

*Graduate Student, Department of Aerospace Engineering, Member AIAA.
†Langley Distinguished Professor, Department of Aerospace Engineering, Associate Fellow AIAA

I. Introduction

ORNITHOPTERS and other flapping-wing unmanned air vehicles have recently become increasingly popular among researchers and hobbyists as miniaturizations in electronics have allowed for the realizations of flapping-wing vehicle designs.[1–4] Ornithopters are aircraft which mimic avian flight mechanics and are typically flown remotely by a ground-based pilot, controlling the flapping rate and the orientation of a tail flap. Ornithopters are interesting and useful flight vehicles due to increases in aerodynamic efficiency over conventional fixed-wing and rotary-wing vehicles in low Reynolds number flows.[5] Additionally it is envisioned that agility and maneuverability similar to that exhibited by birds and insects may be harnessed. Flapping-wing aircraft are well-suited for mission profiles including reconnaissance and wildlife population monitoring, where the aircraft shape and behavior grants a degree of contextual camouflage within the native environment.

The modeling of a flapping wing vehicle is notoriously difficult, in part due to the unsteady, low Reynolds number flows experienced by the vehicle. Several authors have contributed to the understanding of flapping wing aerodynamics, using methods including thin airfoil theory, blade element analysis, and computational fluid dynamics.[6–8] Also the vehicle dynamics are nonlinear and often incorporate several additional degrees of freedom for the wings and other fuselage appendages. Deng et al. used the standard 6 degree of freedom nonlinear aircraft model and incorporated aerodynamics and actuator models to model the flight of a micromechanical flying insect.[9] Sibilski developed a simulation of an entomopter with spherical wing joints using the Gibbs-Appel equations.[10] Wu and Popović generated a realistic simulation using more than 21 degrees of freedom to model the bone and feather movements of a bird.[11] Rashid modeled a full-sized, manned ornithopter as a collection of three rigid bodies using the Newton-Euler dynamics.[12]

The focus of this work is the modeling of the dynamics of an ornithopter with the goal of autonomous flight. The ornithopter was chosen for its ease of flying and the payload capacity for carrying the necessary avionics hardware. The vehicle design results in a significant dependence of the inertial properties on the vehicle pose, which is determined by the wing and tail joint angles. When combining the shifting mass distribution with the extremely quick motions of the ornithopter observed in flight,[13] a multibody model of the ornithopter is needed to achieve fidelity of the dynamics. The ornithopter model is a non-holonomic system, whose equations of motion are commonly derived in space systems, such as spacecraft with additional appendages and manipulators.[14] Specifically, the notation and general representation of the dynamics as presented by Vance[15] and Moosavian[16] is adopted. In this work, the Boltzmann-Hamel equations,[17] otherwise known as the Lagrange equations for quasi-coordinates,[18] are used to form the equations of motion expressed in the fuselage and linkage coordinate frames. While this method requires lengthy computations when compared to other methods,[19] the process is procedural and is easily implemented in symbolic algebra software packages. Additionally the method is flexible to other choices of state variables and vehicle configurations, and is based on scalar energy functions, which are intuitive and may provide future inspiration for Lyapunov functions. The equations are ultimately cast as

$$\mathbf{M}(\mathbf{p})\dot{\mathbf{v}} + \mathbf{C}(\mathbf{p},\mathbf{v})\mathbf{v} + \mathbf{E}(\mathbf{p},\mathbf{v}) = \mathbf{u} \tag{1}$$

which is a canonical form in the literature of the nonlinear robotics and adaptive control communities.[20,21] The vectors $\mathbf{p}$ and $\mathbf{v}$ are the generalized position and velocity states of the system. The matrix $\mathbf{M}(\mathbf{p})$ represents the mass and inertia properties of the system and is a function of the system pose. The matrix $\mathbf{C}(\mathbf{p},\mathbf{v})$ contains the nonlinear dynamic coupling terms, such as centripetal and Coriolis accelerations. The vector $\mathbf{E}(\mathbf{p},\mathbf{v})$ describes the generalized forces imparted on the system by the environment through which it moves, such as the gravitational and aerodynamic effects. The vector $\mathbf{u}$ contains the generalized control forces commanded on the system. Lewis et al. provide a comprehensive list of the properties of these matrices and vectors.[20]

This work begins with an introduction to the ornithopter test bed vehicle and a discussion of the mass properties of the system. Afterwards the schematic of the multibody representation is presented, and the corresponding equations of motion are derived and cast into the form of Equation 1, with notes on the inclusion of gravitational and aerodynamic models. Software implementation of both the symbolic equation derivations and the numerical integration of the equations of motion is discussed. Finally preliminary results are given for a simulation for the case of straight and level flight using a simple aerodynamics model.

II. Aircraft Characterization

The ornithopter used in this study is a modified version of the "Slow Hawk" series of Kinkade ornithopters,[2] shown in Figure 1. The vehicle is piloted remotely using standard hobby radio equipment. One control input commands the speed of a DC motor, which through a gearbox and a four-bar linkage, flaps the wings in unison to produce lift and thrust. Two additional control inputs are used to control servo motors, which pitch and roll linkages in a serial manner to deflect the tail and cause pitching and yawing aerodynamic torques on the vehicle.

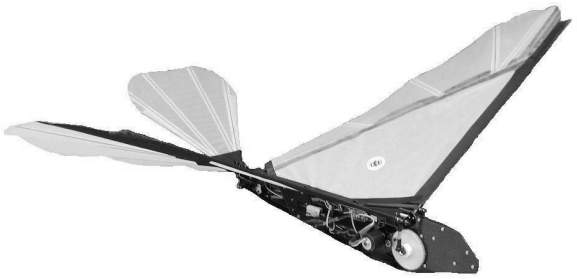

Parameter	Value	Unit
Mass	446.00	g
Length	0.7810	m
Wing Span	1.1960	m
Wing Area	0.3294	m^2
Aspect Ratio	4.3600	-
Mean Chord	0.2950	m

Figure 1. Aircraft and specifications.

The mass and inertia of the individual pieces which comprise the ornithopter can be estimated and combined so that the gross mass distribution can be estimated as a function of the ornithopter pose. Inertia properties for several components such as servo motors and DC motors may be estimated by regarding their geometries as simple shapes. Other components such as the airframe and wings may be computed numerically from their geometries. Then the center of mass and the inertia tensor for the entire system may be computed as

$$\mathbf{r}_{MI} = \sum_i m_i \mathbf{r}_{iI} / \sum_i m_i \tag{2}$$

$$\mathbf{I}_M^M = \sum_i \mathbf{R}^{Mi} \mathbf{I}_i^i \mathbf{R}^{iM} + \sum_i m_i \left(\mathbf{r}_{iM}^T \mathbf{r}_{iM} \mathbb{I} - \mathbf{r}_{iM} \mathbf{r}_i^T \right) \tag{3}$$

by combining the mass m_i and inertia $\mathbf{I}_i$ contributions, measured in frame K_i and transformed to frame K_M. Equation 2 is the position of the gross center of mass relative to an inertial reference, and is a weighted summation of the centers of mass for each of the individual components. Equation 3 is the inertia tensor about the gross center of mass, where the first and second terms rotate and translate the component inertia tensors to the gross center of mass, respectively.

The ornithopter components can be categorized as those which are fixed to the fuselage, those which move with the wings, and those which move with the tail. Of the total mass, the fuselage is 76%, the wings are 19%, and the tail is 5%. To illustrate the variation of the mass distribution, the migration of the gross center of mass and the elements of the inertia tensor, referenced to the center of mass of the fuselage and using conventional aircraft notation,[22] are shown in Figure 2 as a function of the wing angle. Results show a significant change in the vertical location of the center of mass, as well as the inertias along the pitching and yawing directions of the aircraft. This mass distribution, in addition to the large accelerations measured in flight[13] and fast flapping motions of the ornithopter, motivate the use of a multibody model over a conventional single body model for this ornithopter.

III. Model Configuration

The ornithopter is modeled as a system of five interconnected, rigid bodies, as shown in Figure 3 and Figure 4. The system has N degrees of freedom and is comprised of a collection of linkages $1 \leq i \leq N_j$, which form kinematic chains $1 \leq j \leq N_k$ emanating in a tree structure from a central fuselage body. Each linkage rotates with respect to its adjacent inboard linkage through a revolute joint parameterized by an angle θ_{ij} and an axis of rotation $\mathbf{z}_{ij}$. Each linkage has center of mass C_{ij} and coordinate frame K_{ij}, which consists of unit vectors $\{\mathbf{e}_{xij}, \mathbf{e}_{yij}, \mathbf{e}_{zij}\}$. Additionally, vectors $\mathbf{l}_{ij}$ and $\mathbf{r}_{ij}$ describe the locations of the inboard and outboard joint locations, respectively. Estimated mass distribution properties of the linkages are calculated

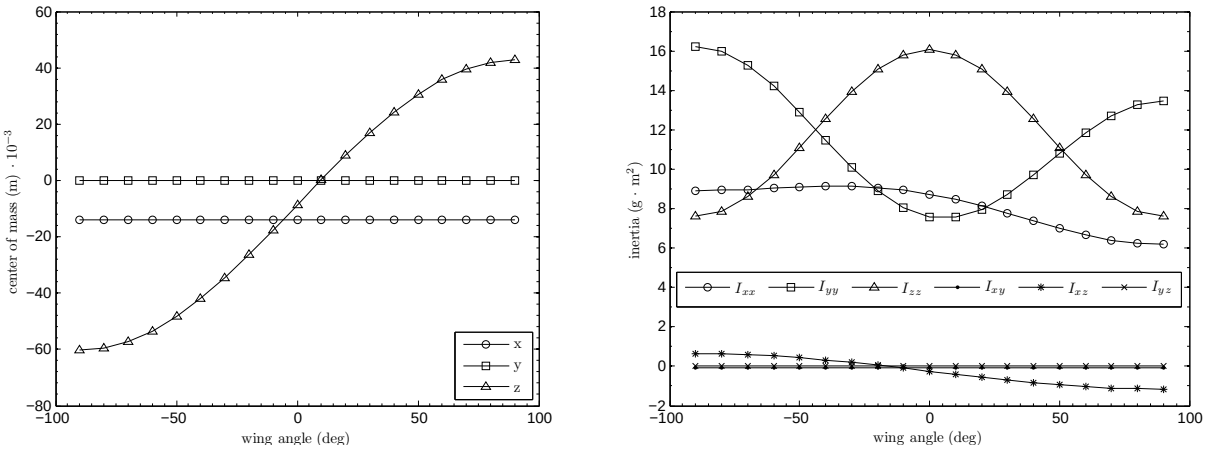

(a) center of mass (b) inertia tensor

Figure 2. Variation of the gross mass distribution over a wing stroke.

using Equations 2 and 3. The first two kinematic chains are the right and left wings, which rotate about the longitudinal axis of the fuselage. The third chain comprises the tail mechanism, which collectively pitches and rolls about the fuselage through two linkages. Additionally an inertial reference is taken at the stationary point C_I fixed to the surface of the Earth, with frame K_I and unit vectors $\{\mathbf{e}_{xI}, \mathbf{e}_{yI}, \mathbf{e}_{zI}\}$ pointing north, east, and down.

The fuselage, represented as body 0, is the base from which all other kinematic chains are attached and is the body in which the system translational and rotational degrees of freedom are expressed. Using the fuselage center of mass as a reference point is called the *direct path method* and provides a more intuitive and algebraically compact set of equations which are more amenable to the inclusion of external forces than other methods, such as the barycentric method.[16] The fuselage has an inertial position $\mathbf{r}$ and an orientation $\boldsymbol{\eta}$, expressed in the inertial frame K_I. The orientation is parameterized by a three or four element vector, for which Hughes[23] and Shuster[24] provide surveys of attitude parameterizations and definitions of associated transforms. The orientation is used to construct a rotation matrix $\mathbf{R}^{0,I}$ to rotate vectors expressed in the inertial frame into the fuselage frame. The translational and rotational velocity of the fuselage are $\boldsymbol{\nu}$ and $\boldsymbol{\omega}$, respectively, and are expressed in the fuselage frame K_0. Expressing the velocities in the fuselage frame parallels the development of the conventional aircraft equations of motion,[22] provides an intuitive formulation of the equations, and expresses the equations in the same frame in which sensor measurements are made. The positions and velocities of the linkages are parameterized in terms of the joint angles θ_{ij} and the joint rates $\dot{\theta}_{ij}$. Using the joint angles and the axes of rotation, rotation matrices $\mathbf{R}^{ij,(i-1)j}$ can be formed to rotate vectors from the adjacent inboard linkage into the linkage frame.

Using the configuration of the system and the body-fixed geometric vectors, the position of a point p on link i of chain j can be written

$$\mathbf{r}_p = \mathbf{r} + \mathbf{r}_{0j} + \sum_{k=1}^{i-1} (\mathbf{r}_{kj} - \mathbf{l}_{kj}) + (\mathbf{r}_{p,ij} - \mathbf{l}_{ij}) \tag{4}$$

where $\mathbf{r}_{p,ij}$ describes the location of the point from the center of mass C_{ij}. Similarly the rotational and translational velocities of the point can be written

$$\boldsymbol{\omega}_{ij} = \boldsymbol{\omega} + \sum_{k=1}^{i} \dot{\theta}_{kj} \mathbf{z}_{kj} \tag{5}$$

$$\boldsymbol{\nu}_p = \boldsymbol{\nu} + \mathbf{S}(\boldsymbol{\omega}) \mathbf{r}_{0j} + \sum_{k=1}^{i-1} \mathbf{S}(\boldsymbol{\omega}_{kj}) (\mathbf{r}_{kj} - \mathbf{l}_{kj}) + \mathbf{S}(\boldsymbol{\omega}_{ij}) (\mathbf{r}_{p,ij} - \mathbf{l}_{ij}) \tag{6}$$

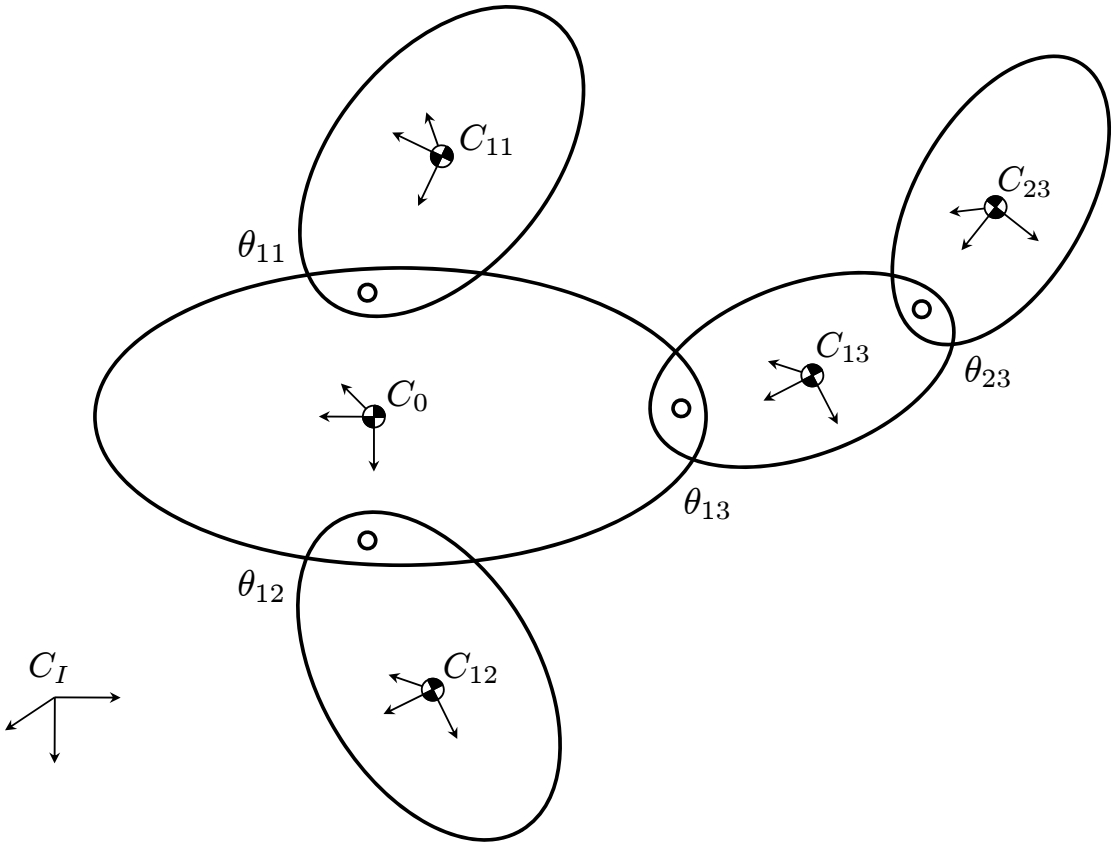

Figure 3. Multibody representation of the ornithopter.

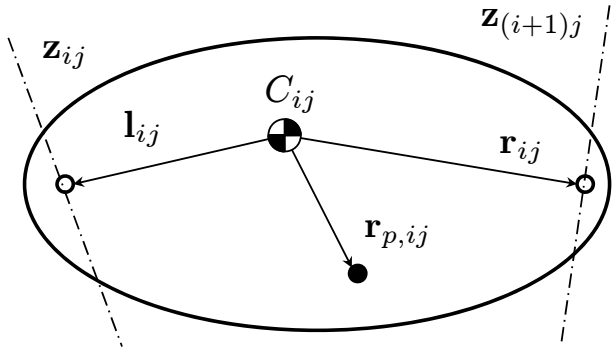

Figure 4. Body-fixed vectors for link i on chain j.

where $\mathbf{S}(.)$ denotes the skew matrix implementation of the cross product operation, which for any two vectors $\mathbf{x}, \mathbf{y} \in \mathbb{R}^{3\times 1}$ is defined

$$\mathbf{x} \times \mathbf{y} = \mathbf{S}(\mathbf{x})\mathbf{y} = \begin{bmatrix} 0 & -x_3 & x_2 \\ x_3 & 0 & -x_1 \\ -x_2 & x_1 & 0 \end{bmatrix} \begin{bmatrix} y_1 \\ y_2 \\ y_3 \end{bmatrix}. \tag{7}$$

Additionally, Equations 4 through 6 can be used to solve for the Jacobian matrices

$$\mathbf{J}_{f,ij} = \begin{bmatrix} \mathbb{I} \\ \mathbf{S}\left[\mathbf{r}_{0j} + \sum_{k=1}^{i-1}(\mathbf{r}_{kj} - \mathbf{l}_{kj}) + (\mathbf{r}_{p,ij} - \mathbf{l}_{ij})\right] \\ \sum_{s=1}^{i}(\mathbf{Z}_{ij})^T\mathbf{S}\left[\sum_{k=s}^{i-1}(\mathbf{r}_{kj} - \mathbf{l}_{kj}) + (\mathbf{r}_{p,ij} - \mathbf{l}_{im})\right] \end{bmatrix} \tag{8}$$

where the matrix

$$\mathbf{Z}_{ij} = \begin{bmatrix} \mathbf{0} & \mathbf{z}_{ij} & \mathbf{0} \end{bmatrix} \tag{9}$$

extracts the generalized torque components on the respective joints. The Jacobian matrices in Equation 8 are used to filter an external force acting at a point $\mathbf{r}_{p,ij}$ to the respective equations for the generalized degrees of freedom.

IV. Equations of Motion

The equations of motion are differential equations which describe how the state variables evolve over time as a function of the current states and the generalized forces. The position and velocity variables of the system are given by

$$\mathbf{p} = \begin{bmatrix} \mathbf{r}^T & \boldsymbol{\eta}^T & \boldsymbol{\theta}^T \end{bmatrix}^T \tag{10}$$

$$\mathbf{v} = \begin{bmatrix} \boldsymbol{\nu}^T & \boldsymbol{\omega}^T & \dot{\boldsymbol{\theta}}^T \end{bmatrix}^T \tag{11}$$

where $\boldsymbol{\theta} = [\theta_{11}, \theta_{12}, \theta_{13}, \theta_{23}]^T$ is a vector of joint angles. The state of the system is then described by a vector concatenating the position and velocity variables

$$\mathbf{x} = \begin{bmatrix} \mathbf{p}^T & \mathbf{v}^T \end{bmatrix}^T. \tag{12}$$

A subset of the equations of motion are the kinematic equations, which describe how the position states evolve in accordance with the velocity states. These state variables are related through the kinematic Jacobian matrix $\mathbf{J}_K^{I,0}$ and are written

$$\begin{bmatrix} \dot{\mathbf{r}} \\ \dot{\boldsymbol{\eta}} \\ \dot{\boldsymbol{\theta}} \end{bmatrix} = \begin{bmatrix} \mathbf{R}^{I,0} & \mathbf{0} & \mathbf{0} \\ \mathbf{0} & \mathbf{J}_\eta^{I,0} & \mathbf{0} \\ \mathbf{0} & \mathbf{0} & \mathbb{I} \end{bmatrix} \begin{bmatrix} \boldsymbol{\nu} \\ \boldsymbol{\omega} \\ \dot{\boldsymbol{\theta}} \end{bmatrix} \tag{13}$$

where the matrix is dependant upon only the orientation of the fuselage. The dimensions and form of this matrix are dependant on the parameterization of the fuselage orientation.

The remaining subset of the equations of motion are the dynamic equations, which describe how the velocity states evolve in accordance with the applied forces. These may be developed using a number of methods, but are derived in this work using the Boltzmann-Hamel equations, which are a generalization of the Lagrange equations, allowing the choice of velocity states that are not strictly the derivative of the position states. In this derivation it is simpler to initially assume the system has no potential energy so that the Lagrangian contains only kinetic energy, and to treat gravity at the end as an external force. The kinetic energy of the system is written

$$T = \frac{1}{2}m_0\boldsymbol{\nu}^T\boldsymbol{\nu} + \frac{1}{2}\boldsymbol{\omega}^T\mathbf{I}_0\boldsymbol{\omega} + \frac{1}{2}\sum_{j=1}^{N_k}\sum_{i=1}^{N_j} m_{ij}\boldsymbol{\nu}_{ij}^T\boldsymbol{\nu}_{ij} + \boldsymbol{\omega}_{ij}^T\mathbf{I}_{ij}\boldsymbol{\omega}_{ij}. \tag{14}$$

which combines the translational and rotational energies of the fuselage and linkages. The equations of motion are then the Boltzmann-Hamel equations, written in matrix form as

$$\frac{d}{dt}\left[\frac{\partial T}{\partial \mathbf{v}}\right]^T + \left(\sum_{k=1}^{N} \frac{\partial T}{\partial v_k}\mathbf{\Gamma}_k\right)\mathbf{v} - \left(\mathbf{J}_K^{I,0}\right)^T \left[\frac{\partial T}{\partial \mathbf{p}}\right]^T = \mathbf{u} \tag{15}$$

where

$$\mathbf{\Gamma}_k = \left(\mathbf{J}_K^{I,0}\right)^T \mathbf{\Lambda}_k (\mathbf{J}_K^{I,0}) \tag{16}$$

and

$$\{\mathbf{\Lambda}_k\}_{ij} = \frac{\partial}{\partial p_j}\{\mathbf{J}_K^{0,I}\}_{ki} - \frac{\partial}{\partial p_i}\{\mathbf{J}_K^{0,I}\}_{kj} \tag{17}$$

form the *Hamel coefficients*, which are skew-symmetric matrices of constants.

Using the fact that the kinetic energy of the system may be written in terms of the generalized mass matrix

$$T = \frac{1}{2}\mathbf{v}^T\mathbf{M}\mathbf{v} \tag{18}$$

and carrying out the partial derivatives in Equation 15, the equations of motion can be written in the form given by Equation 1 as

$$\mathbf{M}\dot{\mathbf{v}} + \left(\dot{\mathbf{M}} + \sum_{k=1}^{N} \frac{\partial T}{\partial v_k}\mathbf{\Gamma}_k - \frac{1}{2}(\mathbf{J}_K^{I,0})^T \left(\mathbb{I} \otimes \mathbf{v}^T\right)\left[\frac{\partial \mathbf{M}}{\partial \mathbf{p}}\right]^T\right)\mathbf{v} = \mathbf{u} \tag{19}$$

where a Kronecker product operator $\otimes$ is used to represent the derivative of the kinetic energy with respect to the position states, which involves a three dimensional tensor.[20,25] The parenthetical expression above forms the dynamic coupling matrix $\mathbf{C}$, which does not have a unique representation. In the adaptive and nonlinear control literature, there is a parameterization where the quantity $\dot{\mathbf{M}} - \mathbf{2C}$ is a skew-symmetric matrix. By extension of the formulation given in Lewis et al.,[20] the dynamic coupling matrix may be chosen as

$$\mathbf{C} = \frac{1}{2}\dot{\mathbf{M}} + \sum_{k=1}^{N} \frac{\partial T}{\partial v_k}\mathbf{\Gamma}_k + \frac{1}{2}\left[\frac{\partial \mathbf{M}}{\partial \mathbf{p}}\right](\mathbf{v} \otimes \mathbb{I})(\mathbf{J}_K^{I,0}) - \frac{1}{2}(\mathbf{J}_K^{I,0})^T(\mathbb{I} \otimes \mathbf{v}^T)\left[\frac{\partial \mathbf{M}}{\partial \mathbf{p}}\right]^T \tag{20}$$

to guarantee this property, as the first term cancels, the second term is defined to be skew-symmetric, the second two terms form the skew-symmetric portion of a matrix, and the summation of skew-symmetric matrices are also skew-symmetric.

At this point we have derived the system matrices $\mathbf{M}$ and $\mathbf{C}$. The remaining term $\mathbf{E}$ describes the generalized forces acting upon the system by the environment in which it moves, which can be decomposed into gravitational and aerodynamic forces. The gravitational forces are found in terms of the potential energy of the system

$$U = -m_0\mathbf{g}^T\mathbf{r} - \sum_{j=1}^{N_k}\sum_{i=1}^{N_j} m_{ij}\mathbf{g}^T\mathbf{r}_{ij} \tag{21}$$

which is a sum of the fuselage and linkage potential energies, where $\mathbf{g}$ is the gravitational acceleration vector. The contribution to the dynamics may then be found by taking the derivative with respect to the position states and transforming the expression into the state variable frames

$$\mathbf{E}_{grav} = (\mathbf{J}_K^{I,0})^T \left[\frac{\partial U}{\partial \mathbf{p}}\right]^T. \tag{22}$$

The aerodynamic forces may also be incorporated. Given a model for how the wings generate lift, drag, and thrust as a function of the position and velocity states, the effect of the resultant aerodynamic forces on each surface $\mathbf{f}_{ij}$ may be combined as

$$\mathbf{E}_{aero} = -\mathbf{J}_{f,0}\mathbf{f}_0 - \sum_{j=1}^{N_k}\sum_{i=1}^{N_j} \mathbf{J}_{f,ij}\mathbf{f}_{ij} \tag{23}$$

where the forces are applied at the aerodynamic centers of each surface. In summary, the full equations of motions form N ordinary differential equations which may be written in the compact form

$$\mathbf{H}(\mathbf{x})\dot{\mathbf{x}} = \mathbf{f}(\mathbf{x}, \mathbf{u}, t). \tag{24}$$

V. Software Implementation

Analytical expressions for the equations of motion for the ornithopter are cumbersome to derive by hand. However, the process is procedural and can easily be programmed into a symbolic algebra program. To this end, the software package Mathematica[26] was selected to generate the equations of motion. The program begins by initializing the system state variables, geometric parameters, inertial parameters, and Jacobian matrices. For the equations to remain globally valid and free of non-physical singularities, a unit quaternion, known also as the set of Euler parameters, is used to represent the fuselage orientation. Positions and velocities of the linkages and the corresponding energies are then computed, followed by the Hamel coefficients. The mass matrix is then found by evaluating the first term in Equation 15 and extracting the coefficients of the generalized acceleration variables. Computation of the dynamic coupling matrix and gravitational effects then follow. The resulting matrices and vectors are simplified and are saved in text files.

Once symbolic expressions are obtained, the equations of motion are numerically integrated to generate state trajectories using MATLAB.[27] The program schematic is shown in Figure 5 and begins by loading configuration files for the ornithopter and specifying initial conditions and function calls. The state equations given by Equation 24 are integrated numerically using the built-in solver `ode15s.m`, which allows for the specification of a state-dependant mass matrix multiplying the state derivatives. After the integration, the state trajectories are saved and are exported to an animation file for visualization.

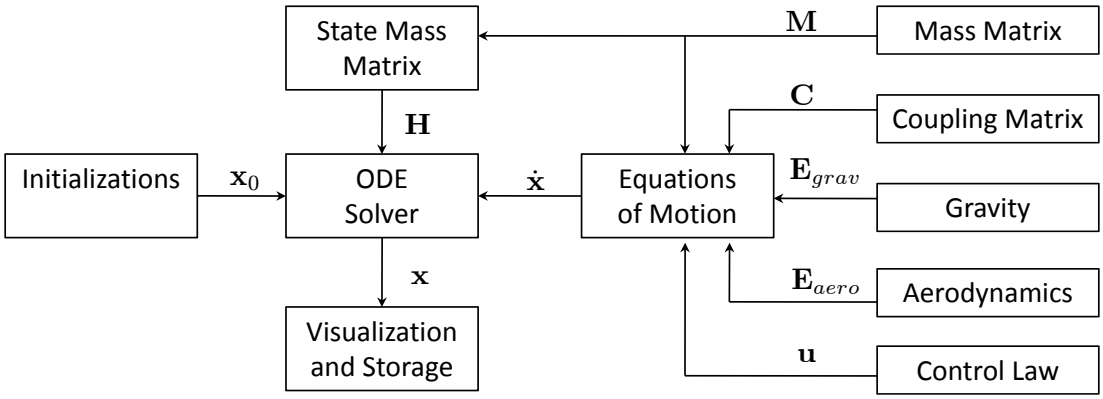

Figure 5. Modular program schematic used to compute state trajectories.

VI. Preliminary Simulation Results

To illustrate the equations of motion, a simulation was performed for the case of straight and level mean flight. In the absence of actuator models for the DC motor and the servo motors dynamics, a feedback-linearization control law with proportional and derivative gains

$$\mathbf{u} = \mathbf{C}\mathbf{v} + \mathbf{E} - \mathbf{M}\left[\mathbf{K}_p(\mathbf{p} - \mathbf{p}_d) + \mathbf{K}_d(\mathbf{v} - \mathbf{v}_d)\right] \tag{25}$$

was used to have the wings synthetically track a sinusoidal flapping pattern and to have the tail remain at a fixed angle. The matrices $\mathbf{K}_p$ and $\mathbf{K}_d$ are positive definite, and the vectors $\mathbf{p}_d$ and $\mathbf{v}_d$ are the desired positions and velocities. Only the control input channels corresponding to the joint angles are applied.

A simple aerodynamics model was used. The lifting bodies are the two wings and the tail flap, each with mean aerodynamic center velocities $\boldsymbol{\nu}_{a,ij}$ and unit vectors pointing in the direction of the thrust, drag, and lift directions as

$$\mathbf{e}_{t,ij} = \frac{\boldsymbol{\nu}_{a,ij}}{\|\boldsymbol{\nu}_{a,ij}\|} \qquad \mathbf{e}_{d,ij} = -\frac{\boldsymbol{\nu}_{a,ij}}{\|\boldsymbol{\nu}_{a,ij}\|} \qquad \mathbf{e}_{l,ij} = \frac{\mathbf{e}_{d,ij} \times \mathbf{e}_{n,ij}}{\|\mathbf{e}_{d,ij} \times \mathbf{e}_{n,ij}\|} \times \mathbf{e}_{d,ij} \tag{26}$$

where $\mathbf{e}_{n,ij}$ is the surface unit normal vector. The thrust, drag, and lift forces acting at the aerodynamic centers are then computed as

$$\mathbf{f}_{t,ij} = \frac{1}{2} C_{t,ij} S_{ij} \rho \|\boldsymbol{\nu}_{a,ij}\|^2 \mathbf{e}_{t,ij} \qquad \mathbf{f}_{d,ij} = \frac{1}{2} C_{d,ij} S_{ij} \rho \|\boldsymbol{\nu}_{a,ij}\|^2 \mathbf{e}_{d,ij} \qquad \mathbf{f}_{l,ij} = \frac{1}{2} C_{l,ij} S_{ij} \rho \|\boldsymbol{\nu}_{a,ij}\|^2 \mathbf{e}_{l,ij} \tag{27}$$

where ρ is the local density of the air and S_{ij} is the surface area. The thrust, drag, and lift coefficients are functions of the local angle of attack

$$\alpha_{a,ij} = \arctan\left(\frac{\mathbf{e}_{zij}^T \boldsymbol{\nu}_{a,ij}}{\mathbf{e}_{xij}^T \boldsymbol{\nu}_{a,ij}}\right) \tag{28}$$

and have been tuned so that the ornithopter flight appears realistic.

The ornithopter is initialized with a fuselage airspeed of 4 m/s and pitch angle of 5 degrees, with the tail pitched at -45 degrees. State trajectories are shown in Figure 6 and a snapshot of the animation in Figure 7. The specified control input keeps the wings and tail angles at their desired values. The resulting pitch angle excursions and pitch rate are about a third of what has been recorded in flight with this ornithopter. However, even with this simple aerodynamics model, the correct trends can be seen in the flight, as the ornithopter remains in the air and undergoes pitching motions as the wings flap.

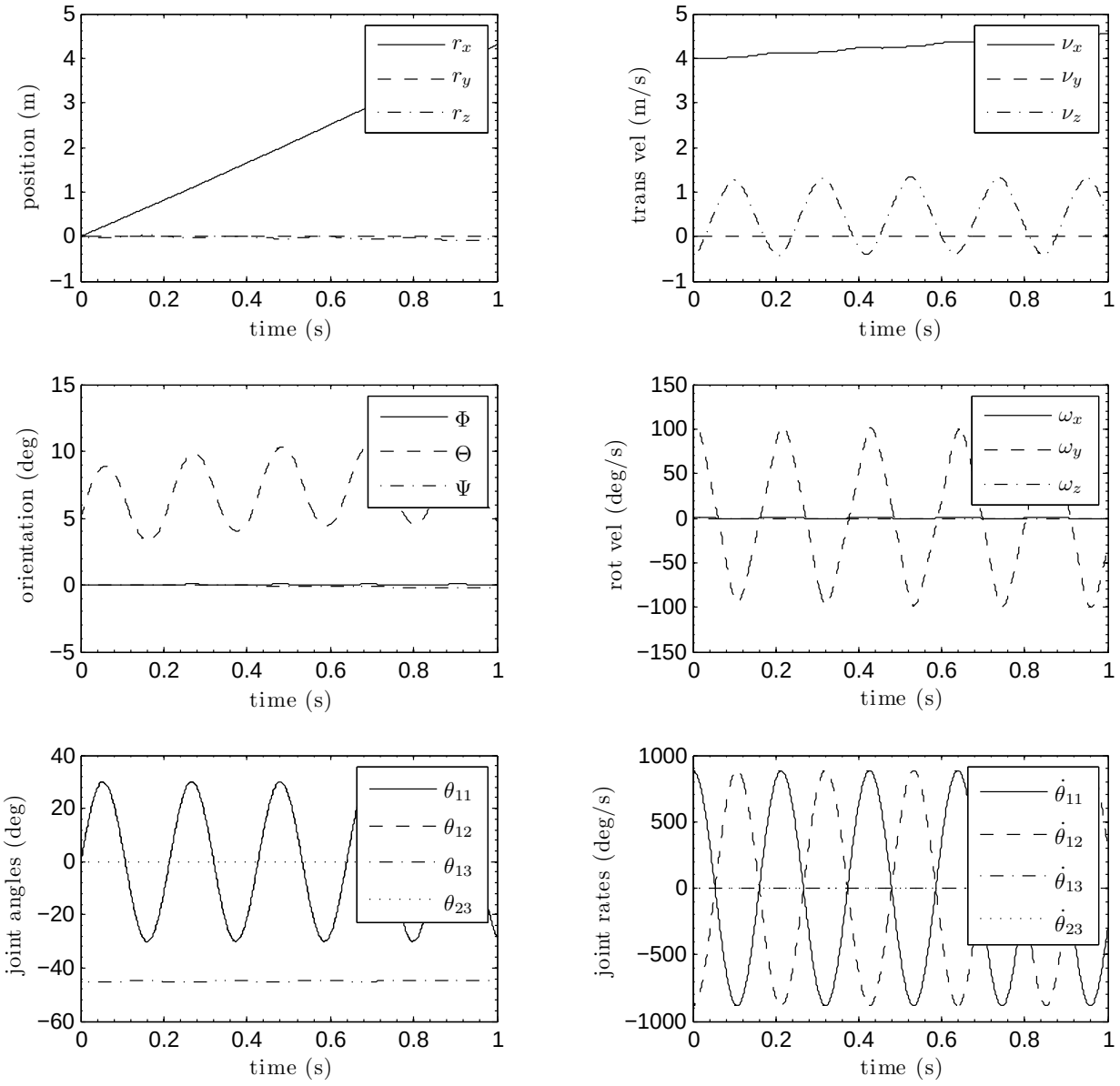

Figure 6. Simulated state trajectories.

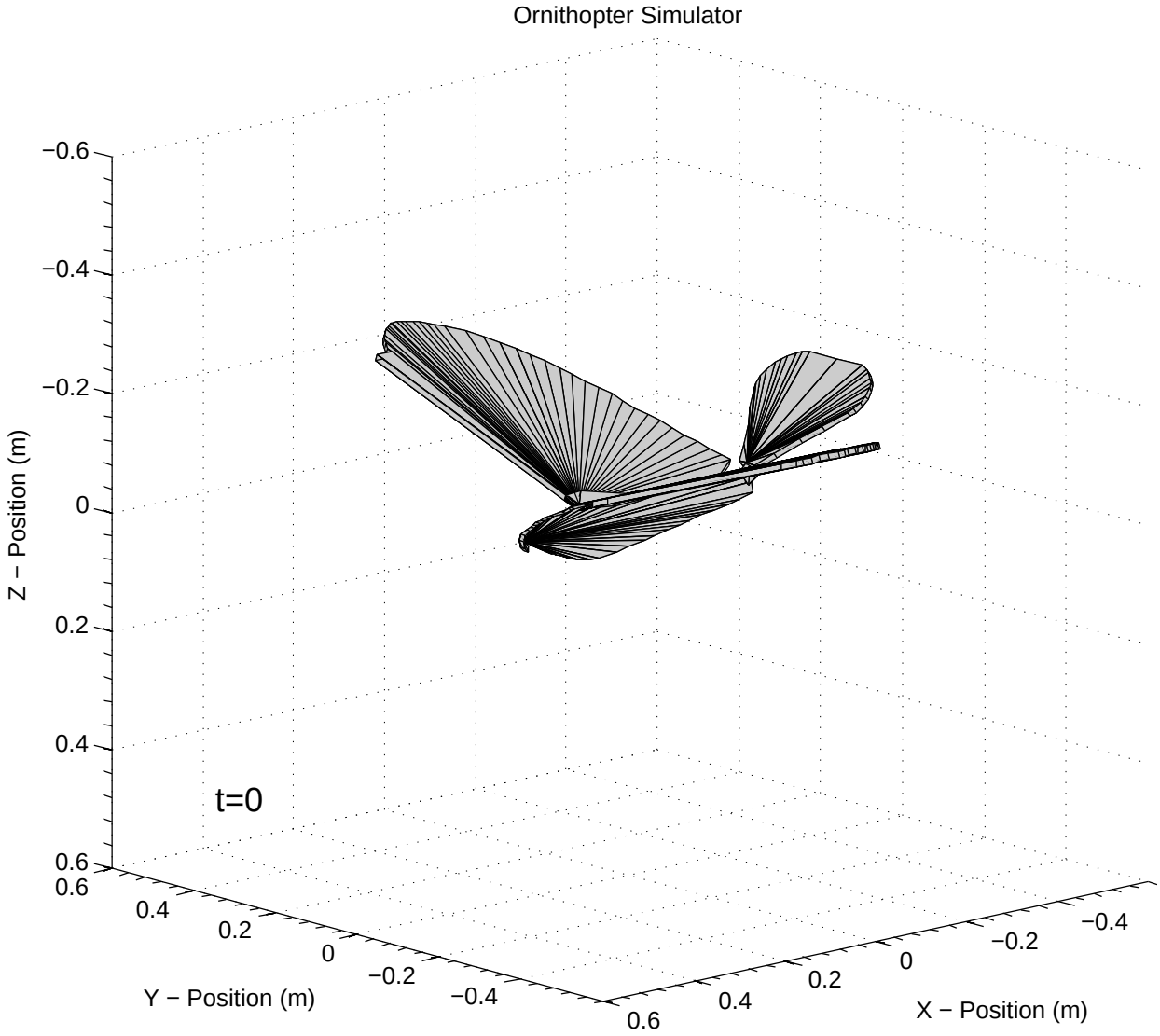

Figure 7. Ornithopter simulator visualization.

VII. Conclusion

This paper presented the derivation of the equations of motion for an ornithopter. Large changes in mass distribution as well as the observation of fast dynamics during flight necessitated the development of a nonlinear multibody model. The equations were derived using the Boltzmann-Hamel equations and were cast in the form convenient for identification and control applications. A simulation was presented for the case of straight and level flight, using a simple aerodynamics model.

VIII. Acknowledgements

The authors would like to thank the University of Maryland, The National Institute of Aerospace, and the NASA Langley Research Center for their support in this research. Several discussions with professors Robert Sanner and Sean Humbert are acknowledged and appreciated. The authors would also like to thank the members of the Morpheus Laboratory for their continued teamwork and motivation, with additional thanks to Nelson Guerreiro for creating the visualization used in the ornithopter simulation.

References

[1]Keennon, M. and Grasmeyer, J., "Development of the Black Widow and Microbat MAVs and a Vision of the Future of MAV Design," No. AIAA Paper 2003-2901, July 2003.

[2]Kinkade, S., "Hobby Technik," www.flappingflight.com, 2008.

[3]Beasley, B., *A Study of Planar and Nonplanar Membrane Wing Planforms for the Design of a Flapping-Wing Micro Air Vehicle*, Master's thesis, University of Maryland, College Park, MD, 2006.

[4]Räbinger, H., "Die Entwicklung der EV-Schlagflügelmodelle," www.ornithopter.de.

[5]Raney, D. and Slominski, E., "Mechanization and Control Concepts for Biologically Inspired Micro Air Vehicles," *Journal of Aircraft*, Vol. 41, No. 6, November - Decemeber 2004, pp. 1257–1265.

[6]Sane, S. and Dickinson, M., "The Aerodynamic Effects of Wing Rotation and a Revised Quasi-Steady Model of Flapping Flight," *Journal of Experimental Biology*, Vol. 205, No. 8, April 2002, pp. 1087–1096.

[7]Harmon, R., Grauer, J., Hubbard, J., and Humbert, S., "Experimental Determination of Ornithopter Membrane Wing Shapes Used for Simple Aerodynamic Modeling," No. AIAA Paper 2008-6397, August 2008.

[8]Roget, B., Sitaraman, J., Harmon, R., Grauer, J., Conory, J., Hubbard, J., and Humbert, S., "A Computational Study of Flexible Wing Ornithopter Flight," No. AIAA Paper 2008-6397, August 2008.

[9]Deng, X., Schenato, L., Wu, W., and Sastry, S., "Flapping Flight for Biomimetic Robotic Insects: Part I - System Modeling," *IEEE Transactions on Robotics*, Vol. 22, No. 4, August 2006, pp. 776–788.

[10]Sibilski, K., "Dynamics of Micro-Air-Vehicle with Flapping Wings," *Acta Polytechnica*, Vol. 44, No. 2, 2004, pp. 15–21.

[11]Wu, J. and Popović, Z., "Realistic Modeling of Bird Flight Animations," *ACM Transactions on Graphics*, Vol. 22, No. 3, July 2003, pp. 888–895.

[12]Rashid, T., *The Flight Dynamics of a Full-Scale Ornithopter*, Master's thesis, University of Toronto, 1995.

[13]Grauer, J. and Hubbard, J., "Inertial Measurements from Flight Data of a Flapping-Wing Ornithopter," *Journal of Guidance, Control, and Dynamics*, Vol. 32, No. 1, January-February 2009, pp. 326–331.

[14]Meirovitch, L. and Kwak, M., "Dynamics and Control of Spacecraft with Retargeting Flexible Antennas," *Journal of Guidance*, Vol. 13, No. 2, March-April 1990, pp. 241.

[15]Vance, E., *Adaptive Control of Free-Floating and Free-Flying Robotic Manipulators*, Ph.D. thesis, University of Maryland, College Park, MD, 1998.

[16]Moosavian, S., *Dynamics and Control of Free-Flying Manipulators Capturing Space Objects*, Ph.D. thesis, McGill University, Montréal, Canada, 1996.

[17]Greenwood, D., *Advanced Dynamics*, Cambridge University Press, 2003.

[18]Meirovitch, L., *Methods of Analytical Dynamics*, McGraw Hill, 1970.

[19]Banerjee, A., "Contributions of Multibody Dynamics to Space Flight: A Brief Review," *Journal of Guidance, Control, and Dynamics*, Vol. 26, No. 3, May-June 2003, pp. 385–394.

[20]Lewis, F., Dawson, D., and Abdallah, C., *Robot Manipulator Control*, Control Engineering Series, Marcel Dekker, 2nd ed., 2004.

[21]Sanner, R., "A Survey of Nonlinear 6DOF Vehicle Control," *ENAE 743: Applied Nonlinear Control of Aerospace Systems* course handouts.

[22]McRuer, D., Ashkenas, I., and Graham, D., *Aircraft Dynamics and Automatic Control*, Princeton University Press, 1973.

[23]Hughes, P., *Spacecraft Attitude Dynamics*, Wiley, 1986.

[24]Shuster, M., "A Survey of Attitude Representations," *The Journal of the Astronautical Sciences*, Vol. 41, No. 4, October-December 1993, pp. 439–517.

[25]Brewer, J., "Kronecker Products and Matrix Calculus in System Theory," *IEEE Transactions on Circuits and Systems*, Vol. 25, No. 9, 1978, pp. 772–781.

[26]Wolfram, "Mathematica," www.wolfram.com, 2008.

[27]MathWorks, T., "MATLAB," www.mathworks.com, 2008.